JOURNAL OF MATERIALS SCIENCE 22 (1987) 2289–2296

Interferometrical measurement of the craze stiffness and structure of the craze fibrils in PMMA

R. SCHIRRER
Institut Charles Sadron (CRM-EAHP), 4, rue Boussingault, 67000 Strasbourg, France

The stiffness of a single craze produced in polymethylmethacrylate (PMMA) at several temperatures at the tip of a running crack has been measured at −25° C and 11 Hz. It has been shown that the craze stiffness increases by a factor of five when the craze is left unloaded during 400 sec at 20° C. A craze produced at 70° C is ten times stiffer than that produced at −25° C. The analogy between the craze structure and an open-cell foam or a crosslinked rubber suggests that the density of "knots" between craze fibrils is a relevant stiffness parameter, and it has been inferred that re-entanglement (welding) occurs between the craze fibrils during the relaxation process and in high-temperature crazes.

1. Introduction

In many instances, new fracture surface formation in polymers is preceded by craze formation. Therefore, the mechanical properties of the craze fibrils (i.e. their rupture) play an essential part in the fracture mechanism. Craze fibrils are made of polymeric material, but compared with bulk material, fibrillar material has some additional characteristics: the surface to volume ratio is extremely high, and the molecules in the fibrils are probably highly oriented. Both features contribute to an increase of the molecular mobility in the fibrils, which may relax faster than ordinary bulk material. On the other hand, the mechanical properties of polymers (tensile modulus, loss factor etc.) are usually dependent on the molecular structure, the molecular weight, and also on the type of entanglement (crosslinking, molecular weight between entanglements). Hence, the mechanical properties are often used to determine the material structure. Very early work on crazing used the mechanical properties of the craze as a means to determine its structure [1–3]. Kambour found that the craze material shows strong non-linear elastic–plastic behaviour and rather low stiffness, comparable to that of a rubber. Once the craze fibrils are completely strain-hardened, he found that the strain against stress curve is linear and reversible, and the stiffness is still low as in a rubber.

From the experimental point of view, several previously published papers have shown that optical interferometry may give information on local mechanical properties in and around the craze at a crack tip [4–7]. Those on craze stiffness have already shown the influence of the molecular weight [8] and of the temperature [8, 9]. The purpose of the present work is to use interferometry to measure the load-opening behaviour of the craze material produced in polymethylmethacrylate (PMMA) (a high molecular weight cast sheet) under various conditions (temperature, relaxation time, velocity etc.) and to try to explain the results in terms of the fibril's structure in the craze. Other recent investigation techniques like transmission electron microscopy (TEM) [10, 11], low-angle electron diffraction (LAED) [12, 13], or small-angle X-ray diffraction (SAXS) [14] may give more direct information on the craze structure, even in real-time experiments under cyclic loading at very low to low frequencies. Nevertheless, these current state-of-the-art techniques restrict the experimental crazing conditions (temperature, frequency, single or multiple crazing, sample thickness etc.), and hence the "easy to use" interferometry gives access to a wider variety of experimental craze production conditions despite other limitations inherent in the wavelength of visible light. The discussion will show that the more direct information on craze structure obtained by SAXS, TEM and LAED, although obtained under other experimental conditions, supports the results shown here.

2. Experimental technique and procedures

Optical interferometry has been widely used and described. The main feature of the technique is that the shape of the craze can be recorded under a wide range of experimental conditions. Fig. 1 shows the well-known relationship between the experimental set-up, the recorded interference fringe pattern and the craze shape deduced from it. The experimental conditions under which the crack/craze system can be propagated and the fringe pattern recorded are: loading frequency from 0 to 500 Hz, sample temperature from −150 to +150° C, crack/craze velocity from 0.01 to 500 $\mu m\,sec^{-1}$. Small compact tension specimens (10 mm × 10 mm × 4 mm) with a single crack/craze are used as described elsewhere [6, 7]. Once the craze is produced at the crack tip under certain conditions, the craze shape as a function of the load applied on the sample is recorded at low load levels.

0022–2461/87 $03.00 + .12

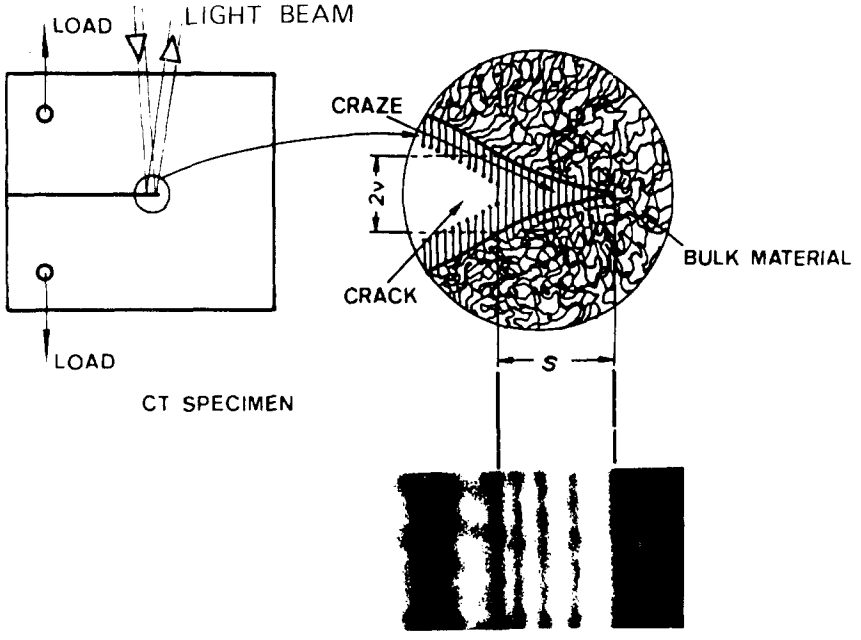

Figure 1 Principle of the interferometrical craze visualization.

Fig. 2 shows the typical craze width ahead of a crack tip against applied load in the case of an increasing load up to fracture. The craze width is calculated from the optical craze width using the Lorentz–Lorenz equation for the optical craze index as a function of its width. The craze index is assumed to be 1.3 for the unloaded case. For low-level loads, the craze opens almost linearly until the fibrils are fully stretched and then the load still increases, but the width does not. Subsequently, the crack propagates. This first result is somewhat different from Kambour's very first measurements [1, 2], where the craze material exhibited strong non-linearity, hysteresis and history dependency. Kambour's craze was produced under quite different conditions (polycarbonate in methanol), and his measurement technique was quite different too. These results correspond rather to Kambour's measurements on a completely strain-hardened craze showing linear elastic behaviour.

Plotting width–load curves measured along one cycle of loading and plotting width–peak load curves obtained from increasing peak amplitude cycles may lead to very different results. In particular, for low frequencies, the structure of the craze may change during the cycle, and may depend on the peak amplitude. Such a dependency has been noted. The residual craze width without load depends particularly on the peak load of the cycle. All measurements in this paper refer to the first case (measurements along one cycle): that is, the fibrils of the craze are always subjected to the same cyclic load, whatever position in the cycle the measurement point is.

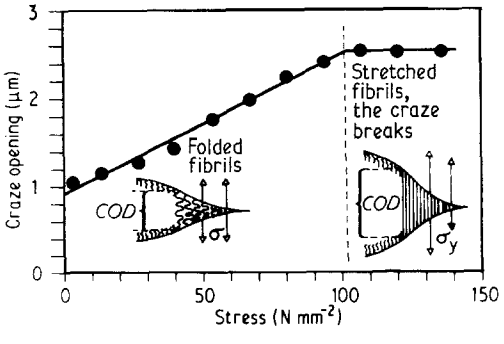

Figure 2 Craze opening against load applied on the sample. The stress shown is the average craze stress from the Dugdale model.

To avoid any fibril rupture and to ensure reproducible results, the craze width was measured under loads never exceeding 50% of the threshold load leading to crack propagation. Ten interference patterns were recorded along the loading cycle, from the bottom of the cycle to the top of the cycle. Fig. 3 shows the shape of an unloaded craze and of the same craze loaded below the threshold. The unloaded craze is taken as a reference and the loaded craze width is then divided by the unloaded craze width. The new drawing simply shows the extension ratio of the loaded craze with respect to the unloaded one. It is almost constant along the whole craze and therefore the craze extension against load curve can be characterized by a single stiffness value from the craze tip to the craze end. This ratio is not the extension ratio of the material in the fibrils, because in the unloaded buckled state, there are still voids between the fibrils. The extension ratio of the fibrils is always higher. As has previously been noticed [1, 2, 9], this craze stiffness is not necessarily the fibril stiffness, but rather the stiffness of the buckled fibrils, which means that the volume fraction of the material, and the fibril diameter and length, are the predominant parameters.

The calculation of the craze stiffness requires knowledge of the stress distribution along the craze boundary. Models to calculate this stress must be used very carefully. The restrictive assumption which is made is that the stress along the craze boundary remains constant from the tip to the end of the craze: it has been shown that this is a good approximation in PMMA except at the very tip, and at the end of the craze for the case of a stretched craze [10, 11, 15]. In the case of a reclosed craze, it is usually admitted that the craze tip is under tension, and the craze end under compression. In our case, Fig. 3 shows that the craze recloses steadily from its tip to its end (the extension

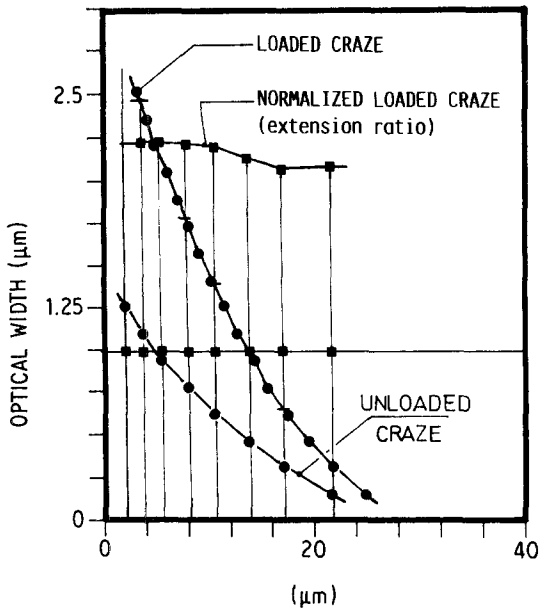

Figure 3 Calculated craze extension with regard to the unloaded craze. The extension ratio is almost the same over the whole craze, and therefore may be defined by a single value for each external load.

from the tip to the end is constant during opening). The stretched craze fits well a constant-stress craze shape (a Dugdale shape) and thus the unloaded one fits it as well. The models to calculate stress distribution along the craze [15] are extremely sensitive to the craze tip position, and the scatter of the calculated stress distribution in our case is too large to claim that the distribution along a closed craze is less constant than along a stretched one. Therefore the stresses used on the plots are simply the K_1 factor divided by the square root of the craze length S:

$$\sigma = \frac{\pi}{8}\frac{K_1}{S^{1/2}}$$

Neither material constants nor volume fraction of the material in the craze are introduced, and hence the calculated stress is proportional but not equal to the stress at the craze fibrils. In the worst case, the loads plotted below in Figs 8, 9 and 10 represent some kind of average value of the local stress over the craze boundary, and hence the craze stiffnesses calculated are some kind of average stiffness over the whole craze volume.

3. Thermal history

Some molecular properties of the craze structure (fibril aspect ratio, structure, entanglement density) play an important role in the mechanical properties (stiffness, loss factor). As these molecular properties may be very sensitive to thermal and mechanical history, a precise measurement protocol must be defined to ensure reproducible and meaningful results. The experiment must be performed in such a way that the stiffness measurement does not change the craze structure previously produced under well-defined conditions. The structure being very sensitive to relaxation, the typical experimental procedure is as follows:

1. A single craze was produced at a running crack tip in a compact tension specimen at 20° C (or perhaps at any temperature from −25 to 70° C), 1.0 μm sec^{-1} crack velocity, under static loading. The craze was kept stretched under a constant load (K_1 just below $K_{1(1\,\mu m\,sec^{-1})}$ and cooled to −25° C. The stress-opening curve of the craze was then measured at 11 Hz. These experimental conditions (11 Hz, −25° C), far below both alpha and beta transitions of the material (PMMA), ensured that the craze structure was not affected by the measurement itself.

2. Another craze produced under the same conditions, instead of being kept stretched during cooling, was left unloaded over a given period of time. Thus the craze fibrils could relax and change their entanglement density. Subsequently the craze was cooled down to −25° C and analysed at 11 Hz as described above.

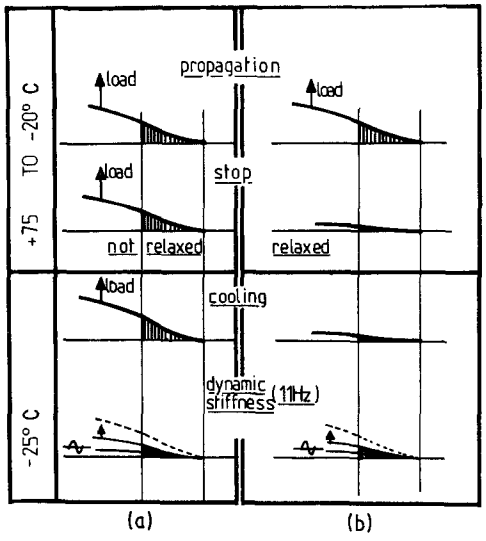

Figure 4 The experimental procedure leading to (a) a "soft" craze (not relaxed), or (b) a "stiff" craze (relaxed). For explanation see text.

Figs 4a and b show the successive steps for both experimental cases and the typical craze stiffness. In Fig. 4a the experimental sequence without relaxation is shown, whereas in Fig. 4b the sequence with relaxation is shown. The final craze stiffnesses are quite different.

Fig. 5 shows the load history of the whole experi-

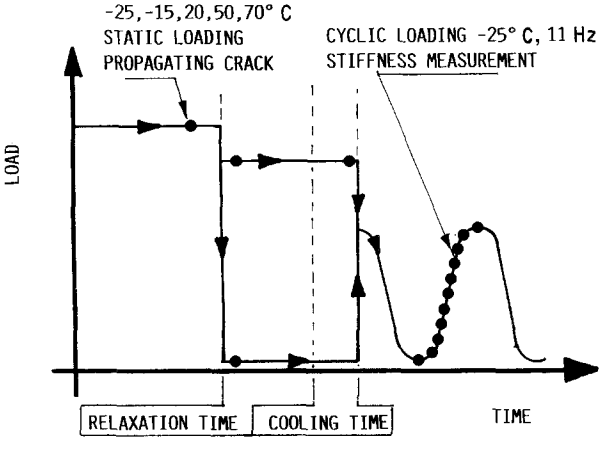

Figure 5 The load–time diagram for both cases (relaxed or non-relaxed craze). The points show the instants when photographs of the interference pattern were taken.

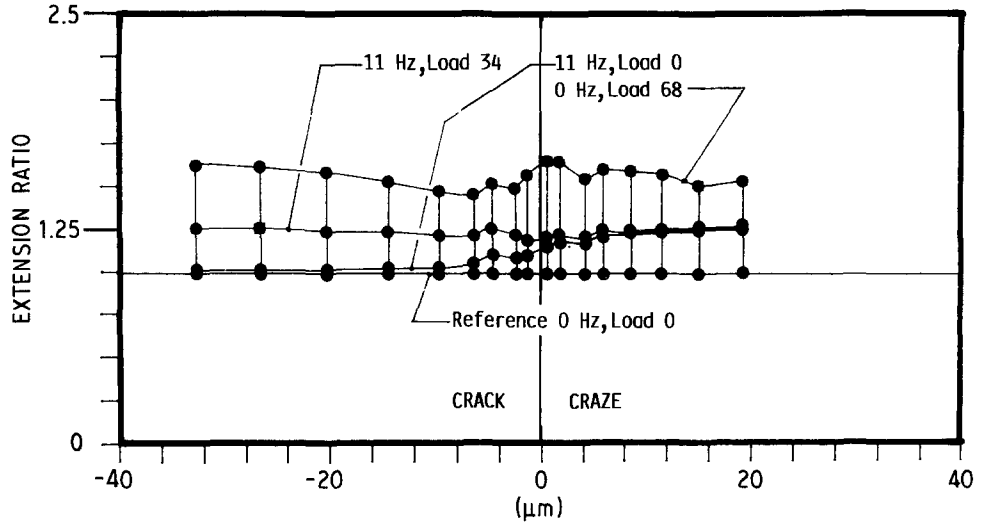

Figure 6 Craze extension ratio as defined in Fig. 3. Note that the craze does not reclose at zero load and 11 Hz, whereas the crack does. All loads in $N\,mm^{-2}$. Case of a rather "stiff" craze. Craze produced at 50° C, not relaxed; measured at −25° C.

ment and the instants at which photographs were taken (the points). The temperature paths with or without relaxation time at zero load are shown.

4. Experimental results

4.1. Crack/craze extension

Fig. 6 shows the extension ratio along the crack and the craze, for a craze that is rather stiff at 11 Hz. From loads of 0 to $34\,N\,mm^{-2}$, the craze does not open, whereas under static loading, crack and craze open identically. Fig. 7 shows a soft craze. It seems that craze material is extremely strain-rate sensitive. Note that at zero load and 11 Hz the craze does not perfectly reclose (this effect is well known), whereas the crack recloses totally.

4.2. Craze load against craze opening

Fig. 8 shows the effect of the two thermal histories described earlier. The craze that was not relaxed opens and recloses almost linearly up to full stretching (there is no difference between the extrapolated 11 Hz full stretching and the static stretching at propagation), whereas the relaxed craze is extremely stiff; the buckled fibrils seem to be welded and will never reach their full extension. During the relaxation the craze shrinks slightly, and its opening reduces from 0.5 to 0.35 μm. If the craze is produced at −25° C (Fig. 9), whether relaxed or not, it behaves in the same way as the non-relaxed one shown in Figs 7 and 8: it seems that there is no relaxation process at −25° C. A craze produced at 50° C (Fig. 10), and not relaxed, is extremely stiff.

4.3. Craze stiffness against relaxation and temperature

Fig. 11 shows the final result of the craze stiffness, for both cases, against the temperature at which the craze was produced. Above 25° C the stiffness increases with temperature for the non-relaxed craze. At a crack propagation velocity of $1\,\mu m\,sec^{-1}$, each fibril stays in the craze for about 30 sec (the craze is about 30 μm long) and for such a short time, relaxation occurs during propagation only if the temperature is above 25° C. In the case of an unloaded craze relaxed for 400 sec, relaxation does not occur below −25° C. This particular temperature (−25° C for PMMA) cor-

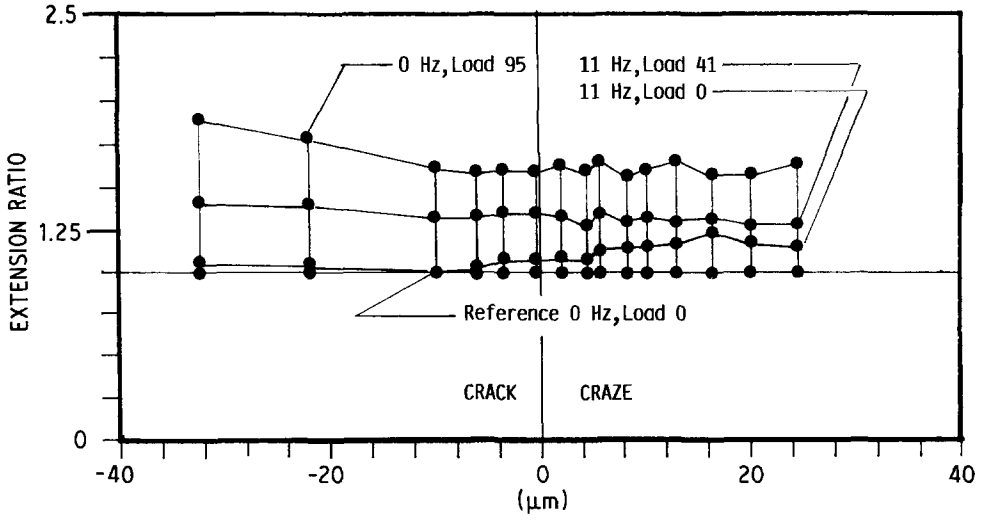

Figure 7 Craze extension ratio in the case of a rather "soft" craze. All loads in $N\,mm^{-2}$. Craze produced at 20° C, not relaxed; measured at −25° C.

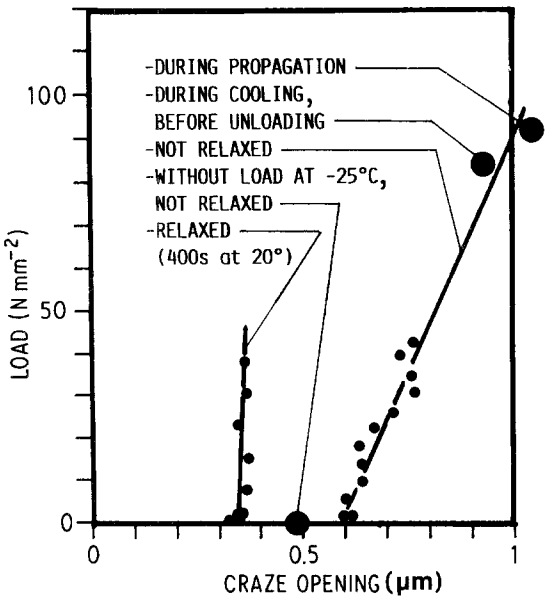

Figure 8 Craze width–load curves for both relaxed and non-relaxed cases for a craze produced at 20° C. Note the stiffness increase after relaxation at 20° C. Craze produced at 20° C; measured at −25° C, 11 Hz. The craze shapes have been fitted with a constant craze stress shape (a Dugdale shape). Crazes with a bad correlation coefficient are omitted. The craze widths shown here and in Figs 9 and 10 are all theoretical openings from the best fit, taken at the same distance from the craze tip for the whole sequence of photographs of the measured craze. This procedure ensures results that can be compared for all photographs.

responds to the critical transition temperature above which the crack propagates with a single craze at its tip, and below which it propagates with a bundle of crazes at its tip.

4.4. Craze stiffness against craze velocity

Fig. 12 shows two values of the stiffness of the crazes created at two different velocities. The craze produced at a higher velocity is less stiff than that produced at a lower velocity. This experiment was somewhat

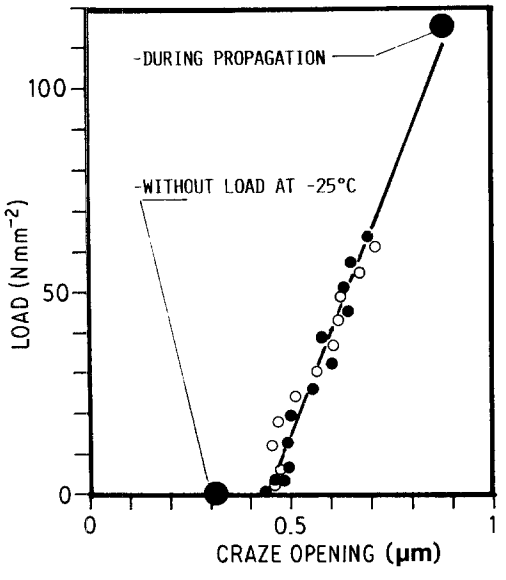

Figure 9 Craze width–load curves for both relaxed and non-relaxed cases for a craze produced at −25° C. Note that there is no stiffness increase at this low relaxation temperature (see also caption to Fig. 8). Craze produced at −25° C; measured at −25° C, 11 Hz. (●) Not relaxed, (○) relaxed.

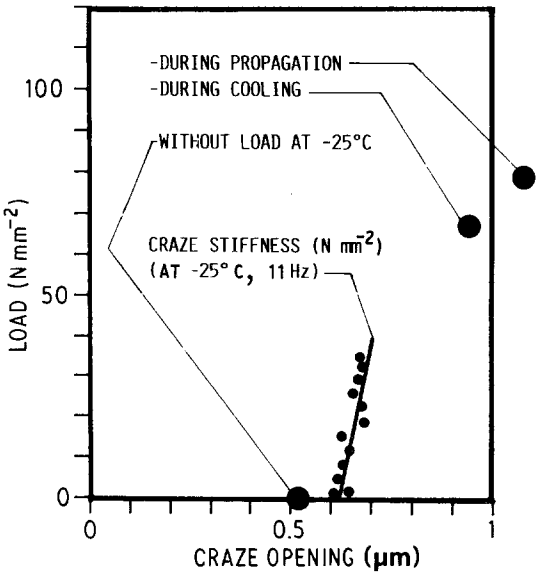

Figure 10 Craze width–load curves for the non-relaxed craze produced at 50° C. Note the high stiffness without relaxation (see also caption to Fig. 8). Craze produced at 50° C, not relaxed; measured at −25° C, 11 Hz.

difficult to conduct, because the craze needed to be stopped after creation, and therefore its velocity went from the maximum velocity to zero, and it is not very clear which velocity has to be considered for the plot, unless the craze was stopped very rapidly so that almost no new craze material was introduced during its deceleration.

5. Discussion

5.1. Discussion of the craze structure

As discussed earlier, the stiffness is not that of the fibrils, but that of the "sponge" of the whole craze (fibrils plus void). This stiffness may vary for three reasons:

(i) Stiffness variation of the material in the fibrils. This effect can only be of minor importance with

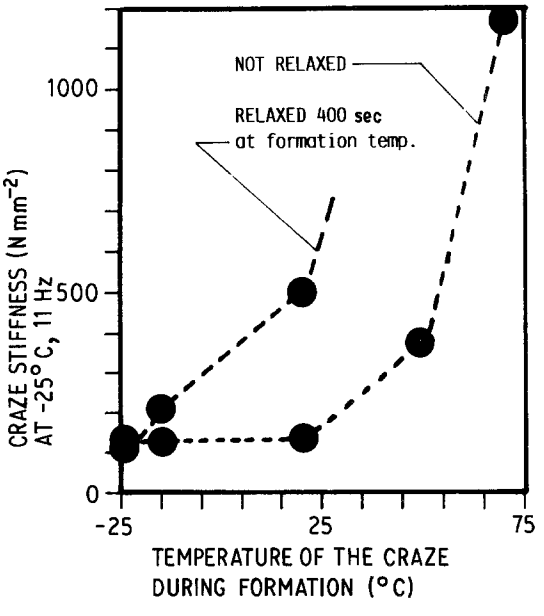

Figure 11 Overall craze stiffness as a function of the temperature at which the craze was produced and as a function of the relaxation.

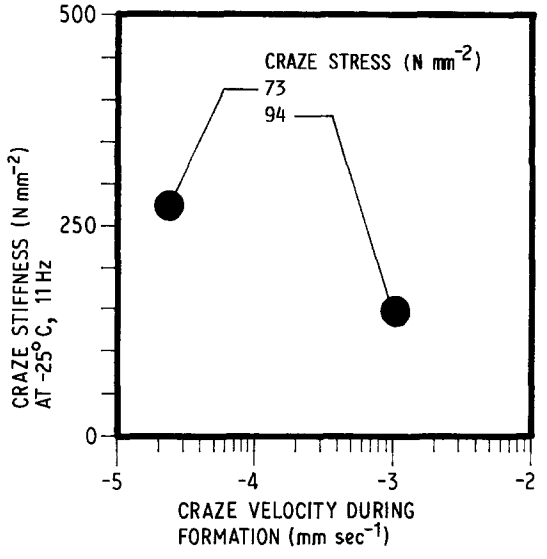

Figure 12 Craze stiffness as a function of the velocity at which the craze was produced. High velocity leads to "soft" crazes.

regard to the stiffness variations obtained here. The polymer itself in the fibrils may only vary its stiffness by a few per cent depending on its thermal history.

(ii) Variation in the shape of the fibrils (diameter/length ratio). It is known that the fibril diameter D varies with the inverse of the fibril stress σ_c under which the fibril was pulled out of the bulk [12, 13, 16, 17]:

$$D\sigma_c = \text{constant} \quad (1)$$

Therefore, fibrils created under high stresses are thinner than those created under low stresses: the fibrils of the rapidly created craze are thinner than those of the slowly created one, and those of a craze created at a high temperature are coarser than those of a craze created at a low temperature. Moreover, during the unloaded relaxation process, the fibrils may thicken by reducing their extremely high orientation [14].

(iii) Variation in the structure of the "sponge" (fewer or more linkages between the fibrils). This might be an important parameter for the craze stiffness, particularly if one takes into account the very high molecular mobility in the craze fibrils which has been extensively discussed by Yang and Kramer [12, 13].

In order to evaluate the craze stiffness, a model describing its structure is needed. The stiffness measurements are performed on a reclosed craze, that is on craze fibrils which are mainly folded. The values of the stiffness are rather low and comparable to that of a rubber. It has also been shown that there are many transverse fibrils connecting the longitudinal fibrils [12, 13, 18–20]. So, the unloaded craze is probably a more or less isotropically buckled bundle of fibrils, as has been noticed by several authors. All these reasons suggest that the craze structure could be compared to two other structures: an open-celled fibrillar "foam" like Gent and Thomas's foam model [21, 22], or a simple partially crosslinked "rubber", in which the craze fibrils stand for "chains" and the junctions between two fibrils stand for "crosslinks". Both models are ultimately inadequate, the first because the fibril volume fraction in the craze is not consistent with the equivalent "foam" stiffness, and the second because the total volume of the craze (fibrils plus voids) is variable during deformation, whereas the volume of a rubbery network is assumed to be constant during deformation. Nevertheless, both types of structure exhibit the same important parameter governing the stiffness: in the foam, it is the square of the length of the fibres between two junctions [21, 22] and in the rubber it is the "chain" (= fibre) length between two "crosslinked" (= junction) points [23]. In terms of density per unit volume of the welded or entangled points between two crossing fibrils, the foam suggests a stiffness scaling proportional to the square of this density, and the rubber suggests a stiffness scaling directly proportional to this density. In any case, at a given fibril diameter (a given fibril flexibility), the most relevant parameter concerning the craze stiffness is the density per unit volume of the welded or entangled fibril crossing points.

There is another argument supporting the model where the real "knots" on the crossing points govern the craze stiffness: if the craze were made of individual fibrils going from one craze boundary to the other one without any other linkage with the other fibrils, the craze stiffness would be that of a bent beam in axial compression. This stiffness is governed by the beam length, which in that case would vary from zero at the craze tip, to the maximum at the craze end. Therefore the craze stiffness would be very high at its tip and very low at its end. This is obviously not the case, as is shown in Fig. 3.

5.2. Discussion of the experimental results

Three experimental parameters have been varied during the craze growth process: velocity, temperature and relaxation time.

5.2.1. Velocity effects

The stress applied on the fibrils in the fast-propagating case is about 94 N mm^{-2}. In the low-speed case it is about 73 N mm^{-2}. Then the fibril diameter ratio for the two cases yields (Equation 1) D(slow)/D(fast) = 0.78. Fig. 12 shows that the stiffness ratio is about 150/275 = 0.55. It can be concluded that the change in stiffness may be mainly due to a change in fibril diameter. Unfortunately, there are no LAED or SAXS experimental results available at different craze propagation velocities to confirm these values.

5.2.2. Temperature effect

Fig. 13 shows the craze stress and the standardized fibril diameter (from Equation 1) associated with the creation of the non-relaxed crazes shown in Fig. 11. From 40 to 70° C the calculated fibril diameter does not vary greatly, whereas, as shown in Fig. 11, the craze stiffness increases drastically. As discussed above, this may be easily explained by an increase in the density of the "welded" crossing points of the fibrils. Depending on the scaling laws mentioned above, the increase from the stiffness at 20° C (100 N mm^{-2}) to the stiffness at 75° C (1000 N mm^{-2}) would correspond to an increase of the "welded" points density of 3 to 10.

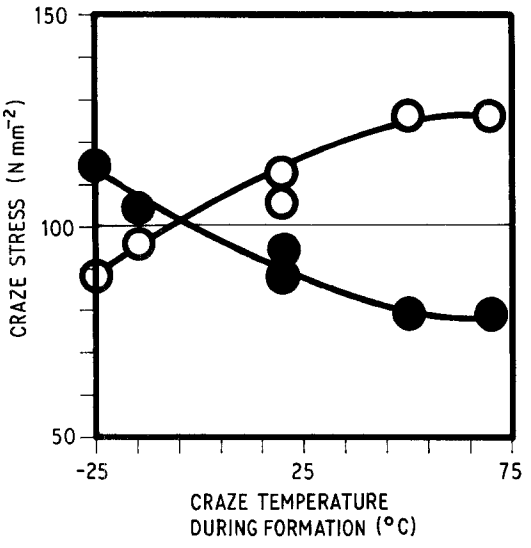

Figure 13 (●) Craze stress (N mm^{-2}) measured during the propagation of the crazes shown in Fig. 11, and (○) the inferred variations (% normalized) of the fibril diameter at the craze formation from Equation 1.

As shown by LAED [12, 13], the craze structure exhibits a quasi-regular arrangement of crosstie fibrils which connect the main fibrils. The results shown here suggest that the density of crosstie fibrils increases when the craze is produced at higher temperature.

5.2.3. Relaxation effect

The stiffness increase during the relaxation process corresponds well to Kambour's first observation: he found that the initial stiffness of an unstressed craze is much higher than the stiffness of the later fully strain-hardened craze. His initial craze was probably relaxed as in our case. During the relaxation process in the unloaded craze, the fibrils may thicken and/or re-entangle at the fibril crossing points as shown in Fig. 14. Other experimental work using LAED [12, 13] showed that the fibrils retract during relaxation, but within a time scale 100 to 10 000 times longer than in our case. Within our 400 sec relaxation time at 20° C, the fibrils practically do not change their diameter. Real-time SAXS [14] showed that the immediate fibril retraction at unloading is about +20% in diameter. A purely thickening mechanism would require a considerable long-distance molecular motion. On the other hand, a purely welded crossing points density increase mechanism would require a density change of about 2 to 5 (foam or rubber scaling law) for the relaxation stiffness increase at 20° C shown in Fig. 11. Welding between fibrils requires much less long-range molecular motion than the thickening mechanism. Therefore it is suggested that the stiffness increase is mainly due to a re-entanglement mechanism at the fibril crossing points, leading to an increase of the "knot" density in the craze structure.

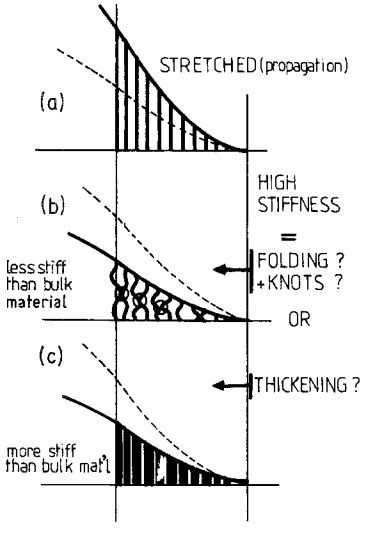

Figure 14 Hypothetical mechanisms of the craze fibril relaxation process. (a) The stretched fibrils during propagation. (b) The folded unloaded fibrils can re-entangle at the points where they cross each other. (c) The folded unloaded fibrils can thicken and shrink, going back to a stretched state.

6. Conclusion

1. The stiffness of crazes has been measured at −25° C and 11 Hz in PMMA. A craze produced at 70° C is ten times stiffer than a craze produced at −25° C. A craze produced at 20° C and unloaded (relaxed) during 400 sec is five times stiffer than a non-relaxed one. A craze produced at −25° C has a stiffness independent of relaxation.

2. The structure of the craze indicates that the craze stiffness is mainly governed by the fibril diameter and the density of welded crossing points between fibrils.

3. The density of welded crossing points can explain the dramatic increase of the craze stiffness for both high-temperature crazes and for relaxed crazes in PMMA. The conclusion is that re-entanglement (welding) occurs between fibrils during the relaxation process. These results are fully in agreement with craze structure observations by low-angle electron diffraction and small-angle X-ray scattering.

The important remaining question concerns the kinetics of the welding of the fibrils. If the craze stiffness is measured at several relaxation times (and not only at 400 sec), the kinetics of the welding may be measured. Then, a reptation model of the molecules in the solid state might be used to determine whether the welding kinetics correspond to a known molecular process. Work using the same kind of approach, connecting the measurement of a mechanical property (fracture toughness) and the molecular diffusion during a welding process, was done earlier in another context [24]. In the case of cyclic craze loading, this type of molecular motion could be of major importance in cyclic fatigue crack propagation, where the temperature–frequency conditions may prevent or permit such re-entanglements. From the fundamental point of view, it implies the rather unusual low-temperature molecular mobility which is now currently admitted by many other authors, and it could be interpreted as some kind of healing at low temperature between the craze fibrils.

References

1. R. P. KAMBOUR, *Polym. Eng. Sci.* **8** (1968) 281.
2. R. P. KAMBOUR and W. KOPP, *J. Polym. Sci. Polym. Phys. Edn.* **7** (1969) 183.
3. J. HOARE and D. HULL, *Phil. Mag.* **(8)26** (1972) 443.

4. R. P. KAMBOUR, *J. Polym. Sci. A2* **4** (1966) 349.
5. H. R. BROWN and I. M. WARD, *Polymer* **14** (1973) 469.
6. W. DOELL, in "Advances in Polymer Science" Vol. 52/53, edited by H. H. Kausch (Springer, Heidelberg, 1983) pp. 105–168.
7. P. TRASSAERT and R. SCHIRRER, *J. Mater. Sci.* **18** (1984) 3004.
8. W. DOELL, *Colloid Polym. Sci.* **256** (1978) 904.
9. R. SCHIRRER and C. GOETT, *J. Mater. Sci. Lett.* **1** (1982) 355.
10. B. D. LAUTERWASSER and E. J. KRAMER, *Phil. Mag.* **A39** (1979) 469.
11. E. J. KRAMER, in "Advances in Polymer Science" Vol. 52/53, edited by H. H. Kausch (Springer, Heidelberg, 1983) pp. 1–56.
12. A. C. M. YANG and A. J. KRAMER, *J. Polym. Sci., Polym. Phys. Edn.* **23** (1985) 1353.
13. *Idem, J. Mater. Sci.* **21** (1986) 3601.
14. P. J. MILLS, E. J. KRAMER and H. R. BROWN, *ibid.* **20** (1985) 4413.
15. W. V. WANG and E. J. KRAMER, *ibid.* **17** (1982) 2013.
16. E. PARADES and E. W. FISCHER, *Makromol. Chem.* **180** (1979) 2707.
17. *Idem, J. Polym. Sci., Polym. Phys. Edn.* **20** (1982) 929.
18. P. BEHAN, M. BEVIS and D. HULL, *J. Mater. Sci.* **8** (1972) 162.
19. *Idem, Phil. Mag.* **24** (1971) 1267.
20. *Idem, Proc. R. Soc.* **A343I** (1975) 525.
21. A. N. GENT and A. G. THOMAS, *Rubber Chem. Tech.* **36** (1963) 597.
22. *Idem, J. Appl. Polym. Sci.* **1** (1959) 107.
23. L. R. G. TRELOAR, "The Physics of Rubber Elasticity" (Clarendon, Oxford, 1975) p. 160.
24. K. JUD, H. H. KAUSCH and J. G. WILLIAMS, *J. Mater. Sci.* **16** (1981) 204.

Received 14 February
and accepted 11 November 1986